

HYBRID CARTESIAN AND ORBIT ELEMENT FEEDBACK LAW FOR FORMATION FLYING SPACECRAFT

Hanspeter Schaub

Sandia National Laboratories, Albuquerque, NM 87185-1003

and

Kyle T. Alfriend

Texas A&M University, College Station, TX 77843

Simulated Reprint from

Journal of Guidance, Navigation and Control

Volume 25, Number 2, March–April, 2002, Pages 387–393



A publication of the
American Institute of Aeronautics and Astronautics, Inc.
1801 Alexander Bell Drive, Suite 500
Reston, VA 22091

HYBRID CARTESIAN AND ORBIT ELEMENT FEEDBACK LAW FOR FORMATION FLYING SPACECRAFT

Hanspeter Schaub *

Sandia National Laboratories, Albuquerque, NM 87185-1003

and

Kyle T. Alfriend †

Texas A&M University, College Station, TX 77843

A spacecraft formation flying control strategy is discussed where the desired orbit is prescribed in terms of specific orbit element differences, and the actual relative orbit is measured in terms of Cartesian coordinates of the rotating chief-satellite-centric reference frame. A direct method to map orbit element differences to their corresponding local Cartesian coordinates is presented. A numerical study illustrates the accuracy at which this transformation performs this coordinate transformation. A hybrid continuous feedback control law is then developed which has the desired relative orbit geometry explicitly given in terms of orbit element differences, and the actual orbit given in terms of local Cartesian coordinates. A numerical simulation illustrates the performance and limitations of such feedback control laws. Using the linearized mapping between the relative orbit coordinates causes only a small performance penalty. However, it is advantageous to work in mean element space when determining the relative orbit tracking error.

Introduction

When describing and controlling spacecraft formations of equal type and built, it is convenient to do so by describing the closed relative orbit geometry in terms of relative orbit element differences, rather than using the relative Cartesian coordinates of the rotating Local-Vertical-Local-Horizon (LVLH) coordinate frame. If the closed relative orbit is a natural solution of the relative orbital mechanics, then the corresponding orbit element difference of the deputy satellite relative to the chief satellite remains constant. Thus, the actual orbit element difference between deputy and chief satellites can be compared at any point of time to their desired values. This greatly facilitates the task of determining any relative orbit errors and correcting them. Establishing relative orbits using mean orbit element differences has been discussed in References 1–4. As a comparison, if a general closed relative orbit is described through some Cartesian initial conditions, then these starting values must be forward integrated to obtain the desired Cartesian coordinates of both the deputy and chief spacecraft. For some special cases it is possible to find closed form solutions to these relative orbits, such as is the case with the elliptic relative orbits obtained using the Clohessy-Wiltshire equations⁵ (sometimes also referred to as Hill's equations). However, these special solutions typically require the chief orbit to be circular and the Earth be perfectly spherical. Using orbit element differences to describe the relative orbit does not suffer from these constraints and is thus more easily applied to the general formation flying problem.

However, a relative orbit is typically sensed or measured in terms of LVLH local coordinates or inertial Cartesian coordinates differences, and typically not directly in terms of orbit element differences. One method to map these local position and velocity measurements into corresponding orbit element differences is to use these local coordinates, along with the inertial chief position and velocity vectors, to reconstruct the deputy inertial position and velocity coordinates. These inertial quantities are then mapped uniquely into corresponding orbit elements which then lead to the desired orbit element differences.

This paper outlines an alternate, more direct approach. Using various celestial mechanics properties, a direct map-

ping between the local Cartesian position and velocity coordinates and the osculating orbit element differences is developed. This transformation is a first order approximation to the true nonlinear transformation, where it is assumed that the relative orbit dimensions are very small compared to the inertial orbits. The good accuracy of this mapping is illustrated through a numerical simulation. Both references 6 and 7 have developed a similar linear mapping between orbit element differences and small differences in relative position and velocity coordinates. The mapping presented in this paper is in terms of orbit elements which lead to non-singular equations for the circular orbit case. While the previous mappings expressed the relative coordinates rates relative to the true latitude angle, we provide direct expressions for the time rate of change of the relative position vector.

Further, a hybrid continuous feedback control law in terms of both the actual local Cartesian relative orbit coordinates and the desired orbit element differences is presented. The linear mapping between local Cartesian coordinates and orbit element differences will provide a direct method to determine the relative orbit errors at any instant without having to forward integrate any desired relative orbit initial conditions. The accuracy and limitation of such a feedback control law are compared to a similar feedback control law, where the full nonlinear transformation between Cartesian local coordinates and their corresponding orbit elements is utilized. Further, the effect of adding the J_2 gravitational perturbation on the tracking accuracy is discussed.

Linear Coordinate Mapping

Since the actual relative orbit of a deputy satellite relative to a chief satellite is typically measured or sensed in terms of LVLH Cartesian coordinates, it would be convenient to be able to map these coordinates directly into corresponding orbit element differences. This would greatly facilitate the process of determining relative orbit errors when the desired relative orbit is provided as fixed orbit element differences.

LVLH Position Coordinates

The rotating LVLH coordinate frame has its x axis aligned with the chief's radial position vector and the z axis aligned with the chief angular momentum vector. Let the LVLH deputy state vector \mathbf{X} be given as

$$\mathbf{X} = (x, y, z, \dot{x}, \dot{y}, \dot{z})^T \quad (1)$$

Let a be the semi-major axis, θ be the true latitude angle (sum of argument of perigee and true anomaly), e be the

*Research Engineer, Sandia National Labs, Albuquerque, NM, AIAA Member.

†Department Head and Professor, Aerospace Engineering Department, Texas A&M University, College Station TX 77843, Fellow AIAA.

Presented as Paper 06-3792 at the AIAA Guidance, Navigation and Control Conference, San Diego, CA, July 29-31, 1996. Copyright ©1996 by the authors. Published by the American Institute of Aeronautics and Astronautics, Inc. with permission.

eccentricity, i be the inclination angle, Ω be the ascending node and ω be the argument of perigee. The orbit element vector \mathbf{e} is given through

$$\mathbf{e} = (a, \theta, i, q_1, q_2, \Omega) \quad (2)$$

with q_1 and q_2 being defined through

$$q_1 = e \cos \omega \quad (3)$$

$$q_2 = e \sin \omega \quad (4)$$

All coordinates are assumed to be osculating quantities with the J_2 perturbation not considered at this stage. Since the relative orbit is small compared to the inertial orbit, the deputy orbit element vector is written as

$$\mathbf{e}_d = \mathbf{e}_c + \delta \mathbf{e} \quad (5)$$

A subscript d denotes deputy spacecraft quantities and a subscript c indicates chief spacecraft quantities. Let us define the following three coordinates systems. Let \mathcal{C} and \mathcal{D} be the LVLH coordinate frame of the chief and deputy satellites respectively, and let \mathcal{N} be the inertial frame. Then $T^{c\mathcal{N}} = T^{c\mathcal{N}}(\Omega_c, i_c, \theta_c)$ is the direction cosine matrix mapping vector components in the inertial frame to components in the chief LVLH frame. To relate the orbit element difference vector $\delta \mathbf{e}$ to the corresponding LVLH Cartesian coordinate vector \mathbf{X} , we write the deputy spacecraft inertial position vector \mathbf{r}_d in chief and deputy LVLH frame components as

$${}^c \mathbf{r}_d = {}^c (R_c + x, y, z)^T \quad (6)$$

$${}^{\mathcal{D}} \mathbf{r}_d = {}^{\mathcal{D}} (R_d, 0, 0)^T \quad (7)$$

where R is the inertial orbit radius. The deputy position vector \mathbf{r}_d is now mapped from deputy LVLH frame vector components to chief LVLH frame vector components using

$${}^c \mathbf{r}_d = T^{c\mathcal{N}} T^{\mathcal{N}\mathcal{D}} {}^{\mathcal{D}} \mathbf{r}_d \quad (8)$$

To simplify the notation from here on, the subscript c is dropped and any parameter without a subscript is implied to be an chief orbit parameter. Taking the first variation of $T^{\mathcal{N}\mathcal{D}}$ and R_d about the chief satellite motion leads to the first order approximations

$$T^{\mathcal{N}\mathcal{D}} \approx T^{\mathcal{N}\mathcal{C}} + \delta T^{\mathcal{N}\mathcal{C}} \quad (9)$$

$$R_d \approx R + \delta R \quad (10)$$

Eq. (8) is then expanded to yield

$${}^c \mathbf{r}_d = (I_{3 \times 3} + T^{c\mathcal{N}} \delta T^{\mathcal{N}\mathcal{C}}) \begin{pmatrix} R + \delta R \\ 0 \\ 0 \end{pmatrix} \quad (11)$$

Dropping second order terms, the deputy position vector is written as

$${}^c \mathbf{r}_d = \begin{pmatrix} R + \delta R \\ 0 \\ 0 \end{pmatrix} + R T^{c\mathcal{N}} \begin{pmatrix} \delta T_{11}^{\mathcal{N}\mathcal{C}} \\ \delta T_{21}^{\mathcal{N}\mathcal{C}} \\ \delta T_{31}^{\mathcal{N}\mathcal{C}} \end{pmatrix} \quad (12)$$

with the matrix components $\delta T_{i1}^{\mathcal{N}\mathcal{C}}$ given by

$$\delta T_{11}^{\mathcal{N}\mathcal{C}} = T_{12}^{\mathcal{N}\mathcal{C}} \delta \theta - T_{21}^{\mathcal{N}\mathcal{C}} \delta \Omega + T_{31}^{\mathcal{N}\mathcal{C}} \sin \Omega \delta i \quad (13)$$

$$\delta T_{21}^{\mathcal{N}\mathcal{C}} = T_{22}^{\mathcal{N}\mathcal{C}} \delta \theta + T_{11}^{\mathcal{N}\mathcal{C}} \delta \Omega - T_{31}^{\mathcal{N}\mathcal{C}} \cos \Omega \delta i \quad (14)$$

$$\delta T_{31}^{\mathcal{N}\mathcal{C}} = T_{32}^{\mathcal{N}\mathcal{C}} \delta \theta + \sin \theta \cos i \delta i \quad (15)$$

Substituting Eqs. (13) - (15) into Eq. (12), the deputy position vector is written in terms of orbit element differences as

$${}^c \mathbf{r}_d = \begin{pmatrix} R + \delta R \\ 0 \\ 0 \end{pmatrix} + R \begin{pmatrix} 0 \\ \delta \theta + \delta \Omega \cos i \\ -\cos \theta \sin i \delta \Omega + \sin \theta \delta i \end{pmatrix} \quad (16)$$

To be able to write Eq. (16) in terms of the desired orbit elements and their differences, the orbit radius R must be expressed in terms of the elements given in Eq. (2).

$$R = \frac{a(1 - q_1^2 - q_2^2)}{1 + q_1 \cos \theta + q_2 \sin \theta} \quad (17)$$

Thus, the variation of R is expressed as

$$\delta R = \frac{R}{a} \delta a + \frac{V_r}{V_t} R \delta \theta - \frac{R}{p} (2aq_1 + R \cos \theta) \delta q_1 - \frac{R}{p} (2aq_2 + R \sin \theta) \delta q_2 \quad (18)$$

where the chief radial and tangential velocity components V_r and V_t are defined as

$$V_r = \dot{R} = \frac{h}{p} (q_1 \sin \theta - q_2 \cos \theta) \quad (19)$$

$$V_t = R \dot{\theta} = \frac{h}{p} (1 + q_1 \cos \theta + q_2 \sin \theta) \quad (20)$$

with h being the chief orbit momentum magnitude and p being the semilatus rectum. Comparing the chief LVLH frame components of the deputy position vector descriptions in Eqs. (6) and (16), the local Cartesian LVLH frame coordinates x , y and z are expressed in terms of the orbit element differences as

$$x = \delta R \quad (21)$$

$$y = R(\delta \theta + \cos i \delta \Omega) \quad (22)$$

$$z = R(\sin \theta \delta i - \cos \theta \sin i \delta \Omega) \quad (23)$$

LVLH Velocity Coordinates

At this point half of the desired mappings between orbit element differences and the corresponding LVLH Cartesian coordinates have been developed. To derive the linear relationship between the orbit element differences and the Cartesian coordinate rates, a similar approach as has been used to derive Eqs. (21) through (23) could be used. In reference 8, the deputy velocity vector is expressed in both the chief and deputy frame. The desired Cartesian coordinate rates are then extracted by comparing the two algebraic expressions.

However, it is also possible to obtain the Cartesian coordinate rate expressions in terms of orbit element differences by differentiating Eqs. (21) through (23) directly with respect to time. The only time varying quantities in these three expressions are the chief true latitude θ and the difference between deputy and chief latitude $\delta \theta$. Only the later quantity needs special consideration. Using the conservation of angular momentum h , we express the true latitude rate $\dot{\theta}$ as

$$\dot{\theta} = \frac{h}{R^2} \quad (24)$$

The variation of Eq. (24) yields

$$\delta \dot{\theta} = \frac{\delta h}{R^2} - 2 \frac{h}{R^3} \delta R \quad (25)$$

Using the angular momentum expression $h = \sqrt{\mu p}$, the δh variation is expressed as

$$\delta h = \frac{h}{2p} \delta p \quad (26)$$

where δp is given by

$$\delta p = \frac{p}{a} \delta a - 2a(q_1 \delta q_1 + q_2 \delta q_2) \quad (27)$$

Thus the desired variation in the true latitude rate is expressed as

$$\delta\dot{\theta} = \frac{h}{R^2} \left(\frac{\delta p}{2p} - 2 \frac{\delta R}{R} \right) \quad (28)$$

After differentiating Eqs. (21)-(23) and making use of Eq. (28), the Cartesian coordinate rates are expressed in terms of orbit element differences as

$$\begin{aligned} \dot{x} = & -\frac{V_r}{2a} \delta a + \left(\frac{1}{R} - \frac{1}{p} \right) h \delta \theta \\ & + (V_r a q_1 + h \sin \theta) \frac{\delta q_1}{p} + (V_r a q_2 - h \cos \theta) \frac{\delta q_2}{p} \end{aligned} \quad (29)$$

$$\begin{aligned} \dot{y} = & -\frac{3V_t}{2a} \delta a - V_r \delta \theta + (3V_t a q_1 + 2h \cos \theta) \frac{\delta q_1}{p} \\ & + (3V_t a q_2 + 2h \sin \theta) \frac{\delta q_2}{p} + V_r \cos i \delta \Omega \end{aligned} \quad (30)$$

$$\begin{aligned} \dot{z} = & (V_t \cos \theta + V_r \sin \theta) \delta i \\ & + (V_t \sin \theta - V_r \cos \theta) \sin i \delta \Omega \end{aligned} \quad (31)$$

Non-Dimensional Cartesian Coordinates

Even the feedback control law discussed in this paper requires the dimensional relative Cartesian coordinates and associated time rates, in some applications it is more convenient to work with non-dimensional quantities. Let (u, v, w) be the non-dimensional relative Cartesian coordinates. Dividing Eqs. (21)-(23) by the orbit radius R , they are defined as:

$$\begin{aligned} u = \frac{x}{R} = & \frac{\delta a}{a} + \frac{V_r}{V_t} \delta \theta - (2a q_1 + R \cos \theta) \frac{\delta q_1}{p} \\ & - (2a q_2 + R \sin \theta) \frac{\delta q_2}{p} \end{aligned} \quad (32)$$

$$v = \frac{y}{R} = \delta \theta + \cos i \delta \Omega \quad (33)$$

$$w = \frac{z}{R} = \sin \theta \delta i - \cos \theta \sin i \delta \Omega \quad (34)$$

Instead of differentiating (u, v, w) with respect to time, we choose to use the true latitude angle θ as the time dependent variable. Let a prime symbol indicate a derivative with respect to θ . To differentiate the expressions in Eqs. (32)-(34), only the $\delta\theta$ terms must be given special consideration. Note that

$$\frac{\partial(\delta\theta)}{\partial\theta} \frac{d\theta}{dt} = \delta\theta' \dot{\theta} = \delta\dot{\theta} \quad (35)$$

Using Eq. (28), the partial derivative of $\delta\theta$ with respect to the true latitude is given by:

$$\delta\theta' = \frac{\delta p}{2p} - 2u \quad (36)$$

Taking the partial derivative of Eqs. (32)-(34) while making use of Eq. (36) yields the following non-dimensional rate

with respect to true latitude.

$$\begin{aligned} u' = & -\frac{3}{2} \frac{V_r}{V_t} \frac{\delta a}{a} \\ & + \left(\frac{R}{p} (q_1 \cos \theta + q_2 \sin \theta) - \left(\frac{V_r}{V_t} \right)^2 \right) \delta \theta \\ & + (3V_r a q_1 + R V_t \sin \theta + R V_r \cos \theta) \frac{\delta q_1}{p V_t} \\ & + (3V_r a q_2 + R V_t \cos \theta - R V_r \sin \theta) \frac{\delta q_2}{p V_t} \end{aligned} \quad (37)$$

$$\begin{aligned} v' = & -\frac{3}{2} \frac{\delta a}{a} - 2 \frac{V_r}{V_t} \delta \theta \\ & + (2R \cos \theta + 3a q_1) \frac{\delta q_1}{p} \\ & + (2R \sin \theta + 3a q_2) \frac{\delta q_2}{p} \end{aligned} \quad (38)$$

$$w' = \cos \theta \delta i + \sin \theta \sin i \delta \Omega \quad (39)$$

Note that these non-dimensional rates expressions are not simpler than their dimensional counterparts. To map these rates with respect to true latitude into the corresponding dimensional (x, y, z) time rates, the following equations are used.

$$\dot{x} = V_t u' + V_r u \quad (40)$$

$$\dot{y} = V_t v' + V_r v \quad (41)$$

$$\dot{z} = V_t w' + V_r w \quad (42)$$

Linear Mapping Accuracy

Combined, Eqs. (21) - (23) and (29)-(31) provide a direct first order mapping of orbit element differences into corresponding LVLH Cartesian coordinates. These six equations are written in matrix form as

$$\mathbf{X} = A(e) \delta e \quad (43)$$

where the 6×6 matrix $A(e)$ is the linear mapping between the two coordinate sets. To obtain the inverse transformation, the six equations can be solved for δe in terms of the \mathbf{X} components to yield

$$\delta e = A(e)^{-1} \mathbf{X} \quad (44)$$

Since this inverse mapping is not used in this paper, it has not been included. However, it can be found in the Appendix of Reference 9.

The following numerical study illustrates what level of errors are introduced to the LVLH Cartesian coordinates when the linear mapping in Eq. (43) is used. Given the chief orbit elements shown in Table 1, specific sets of orbit element differences are used to compute the corresponding LVLH Cartesian position and velocity coordinates.

Table 1 Chief Orbit Elements

Orbit Elements	Value	Units
a	7555	km
e	0.05	
i	48.0	deg
Ω	20.0	deg
ω	10.0	deg
M	120.0	deg

A semi-major axis, eccentricity, inclination angle, ascending node, argument of perigee and mean anomaly difference is prescribed individually for each test run. The orbit element differences are swept from zero to a value which corresponds to a relative orbit having a maximum radius of approximately 1 kilometer. The results are shown in Figure 1.

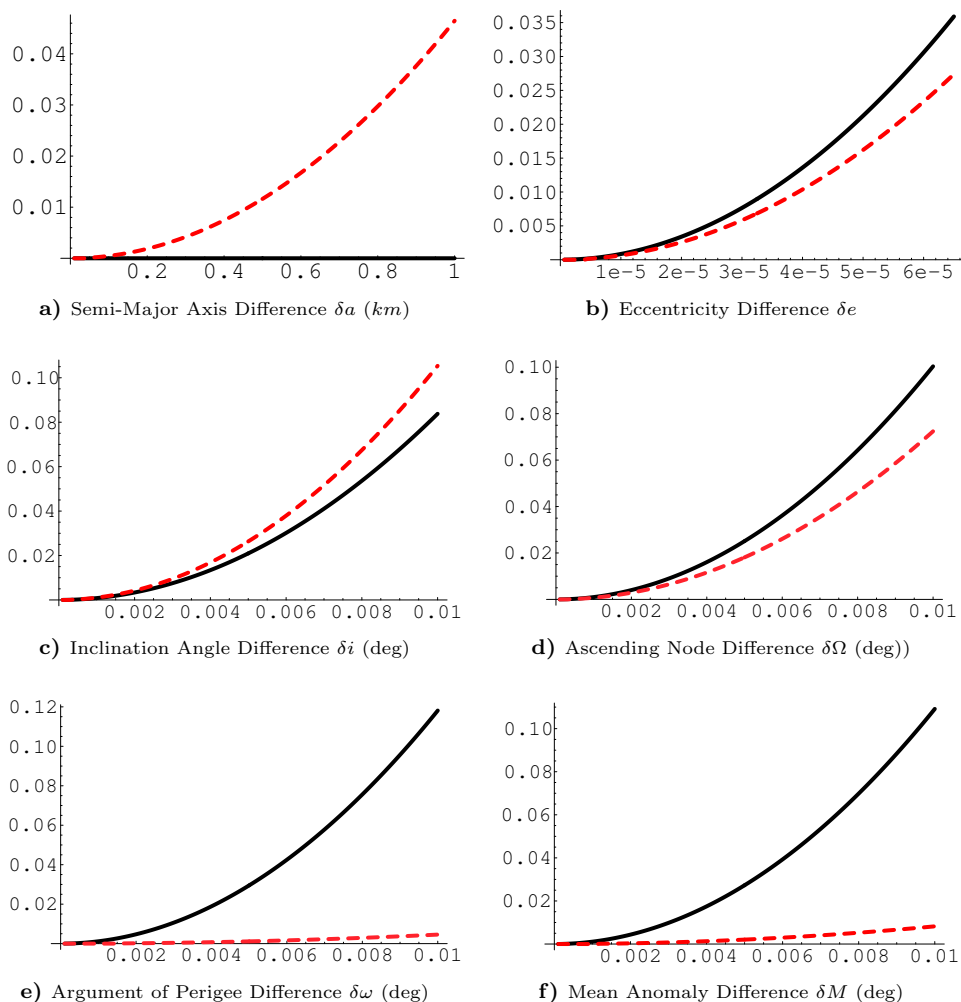


Fig. 1 RMS Errors of the Linear Transformation Matrix $A(e)$ Mapping Orbit Element Differences to LVLH Cartesian Position (solid line in m) and Velocity (dashed line in mm/s) Coordinates

Note that the semi-major axis causes essentially no transformation errors in the position magnitudes. This result is easily verified analytically. With only the orbit element difference δa being non-zero for this case, using Eqs. (21) - (23) we find

$$|\mathbf{x}| = \frac{R}{a} \delta a \quad (45)$$

The chief orbit radius R_c is given by

$$R_c = a_c(1 - e_c \cos E_c) \quad (46)$$

with E_c being the chief eccentric anomaly. The deputy radius vector is expressed as

$$R_d = (a_c + \delta a)(1 - e_c \cos E_c) = R_c + \frac{R}{a} \delta a \quad (47)$$

since only the semi-major axis is different between chief and deputy satellites for this special case. Here the x coordinate is simply the difference in orbit radii. Thus the true position vector magnitude is the same as the one predicted by the linear transformation in Eq. (45).

The remaining RMS position or velocity errors grow only up to 0.1 m or mm/s respectively. Considering that for the largest orbit element differences considered here the relative orbit has a radius of about 1 km with relative velocity magnitudes in the meters range, these transformation errors are very small at typically less than 0.1 %.

Note that the transformation errors shown are not meant to provide a global bound on the mapping errors. These

errors would depend on the chief orbit itself and on at which orbit latitude angle they were evaluated. However, for the given chief orbit with a desired inclination angle difference of the order of 0.01 degrees, this study shows that any control law that utilizes the linear mapping in Eq. (43) could only expect a final position tracking error of about 0.1 meter under the best of circumstances. Using the $A(e)$ mapping instead of the precise nonlinear mapping will result in a small performance loss.

Continuous Feedback Law

Various feedback laws have been proposed for the spacecraft formation flying control task. In Reference 10, continuous feedback laws are presented in terms of mean orbit element tracking errors and mean inertial Cartesian coordinates tracking errors. Reference 11 presents an impulsive feedback law in terms of mean orbit elements. References 12 and 13 present continuous feedback laws in terms of Cartesian coordinates, and Reference 14 discusses a feedback law in terms of orbit elements.

The use of Eq. (43) is investigated here to create a hybrid continuous feedback control law in terms of Cartesian LVLH frame coordinates, while describing the desired relative orbit geometry through a desired set of orbit element differences $\delta \mathbf{e}^*$. Any desired states are denoted in this paper with a superscript asterisk. The advantage of this type of hybrid control law is that the actual relative orbit is expressed in terms of coordinates in which it would actually be measured (i.e. the chief frame local LVLH coordinates), while the desired relative orbit is conveniently expressed as a set of orbit element differences.

Let $\mathbf{x} = (x, y, z)^T$ be the deputy position vector and $\mathbf{v} = (\dot{x}, \dot{y}, \dot{z})^T$ be the deputy velocity vector expressed in the chief LVLH frame. The general linearized relative equations of motion for a Keplerian system are expressed as¹⁵

$$\begin{aligned} \dot{\mathbf{x}} &= \mathbf{v} & (48) \\ \dot{\mathbf{v}} &= \underbrace{\begin{bmatrix} 2\frac{\mu}{R^3} + \dot{\theta}^2 & \ddot{\theta} & 0 \\ -\ddot{\theta} & \dot{\theta}^2 - \frac{\mu}{R^3} & 0 \\ 0 & 0 & -\frac{\mu}{R^3} \end{bmatrix}}_{A_1} \mathbf{x} \\ &+ \underbrace{\begin{bmatrix} 0 & 2\dot{\theta} & 0 \\ -2\dot{\theta} & 0 & 0 \\ 0 & 0 & 0 \end{bmatrix}}_{A_2} \mathbf{v} + \underbrace{\begin{pmatrix} u_x \\ u_y \\ u_z \end{pmatrix}}_{\mathbf{u}} \end{aligned} \quad (49)$$

These relative equations of motion are valid for both circular and elliptic chief orbits. The latitude acceleration is computed through

$$\ddot{\theta} = -2\frac{\mu}{R^3}(q_1 \sin \theta - q_2 \cos \theta) \quad (50)$$

Let us define the relative orbit tracking errors as

$$\Delta \mathbf{x} = \mathbf{x} - \mathbf{x}^* \quad (51)$$

$$\Delta \mathbf{v} = \mathbf{v} - \mathbf{v}^* \quad (52)$$

with the desired position and velocity vectors computed using

$$\mathbf{X}^* = \begin{pmatrix} \mathbf{x}^* \\ \mathbf{v}^* \end{pmatrix} = A(\mathbf{e})\delta \mathbf{e}^* \quad (53)$$

Note that if the desired orbit element differences call for a fixed mean anomaly difference, as is done in References 1, 10 and 11, then the vector $\delta \mathbf{e}^*$ is not constant, but rather $\delta \theta$ must be computed at each instant by solving Kepler's equation. Further, note that $\Delta \dot{\mathbf{x}} = \Delta \mathbf{v}$.

Let us define the control law \mathbf{u} as

$$\mathbf{u} = \dot{\mathbf{v}}^* - A_1 \mathbf{x} - A_2 \mathbf{v} - K \Delta \mathbf{x} - P \Delta \mathbf{v} \quad (54)$$

with K and P being positive definite matrices. To prove that \mathbf{u} is asymptotically stabilizing, a positive definite Lyapunov function V is defined as

$$V(\Delta \mathbf{x}, \Delta \mathbf{v}) = \frac{1}{2} \Delta \mathbf{v}^T \Delta \mathbf{v} + \frac{1}{2} \Delta \mathbf{x}^T K \Delta \mathbf{x} \quad (55)$$

Substituting Eqs. (49) and (52), the derivative of V along the state trajectory must be negative semi-negative

$$\dot{V} = \Delta \mathbf{v}^T (\Delta \dot{\mathbf{v}} + K \Delta \mathbf{x}) = -\Delta \mathbf{v}^T P \Delta \mathbf{v} \quad (56)$$

which guarantees that \mathbf{u} is globally stabilizing. To proof that the control law is also asymptotically stabilizing, the higher order time derivatives of V are investigated. The second derivative of V is zero when evaluated on the set where $\dot{V} = 0$. The third derivative

$$\ddot{V}(\Delta \mathbf{v} = 0) = -2 \Delta \mathbf{x}^T K P K \Delta \mathbf{x} \quad (57)$$

is negative definite in the state vector $\Delta \mathbf{x}$. Since this first non-zero derivative is an odd derivative, the control \mathbf{u} is asymptotically stabilizing.¹⁶

Note that $\dot{\mathbf{v}}^* - A_1 \mathbf{x}^* - A_2 \mathbf{v}^*$ is zero if the desired relative motion is a natural solution to the linearized equations of motion shown in Eq. (49). Assuming that our chosen $\dot{\mathbf{v}}^*$ abides by

$$\dot{\mathbf{v}}^* = A_1 \mathbf{x}^* + A_2 \mathbf{v}^* \quad (58)$$

the control law \mathbf{u} is written as

$$\mathbf{u} = - \begin{bmatrix} A_1 + K & 0_{3 \times 3} \\ 0_{3 \times 3} & A_2 + P \end{bmatrix} \left(\begin{pmatrix} \mathbf{x} \\ \mathbf{v} \end{pmatrix} - A(\mathbf{e})\delta \mathbf{e}^* \right) \quad (59)$$

Note however that the desired relative motion must not necessarily be a natural solution. The control law in Eq. (54) is also valid for forced relative orbits. Studying this form of control law in Eq. (59), the hybrid nature of \mathbf{u} is evident in that the desired relative orbit is prescribed through a set of orbit element differences, while the actual motion is expressed in terms of the chief LVLH frame Cartesian components. The advantage here is that we are able to express the actual and desired relative motion in coordinates which best suit their task.

Since the A_2 matrix is skew-symmetric, it could be dropped from the control expression in Eq. (59). The Lyapunov based stability proof remains the same and asymptotic stability is still guaranteed. However, computing \dot{V} the term $\Delta \mathbf{v}^T A_2 \Delta \mathbf{v}$ is dropped since it is always zero. The modified control expression is then

$$\mathbf{u} = - \begin{bmatrix} A_1 + K & 0_{3 \times 3} \\ 0_{3 \times 3} & P \end{bmatrix} \left(\begin{pmatrix} \mathbf{x} \\ \mathbf{v} \end{pmatrix} - A(\mathbf{e})\delta \mathbf{e}^* \right) \quad (60)$$

This control would no longer feedback linearize the closed loop dynamics, but it still guarantees asymptotic stability.

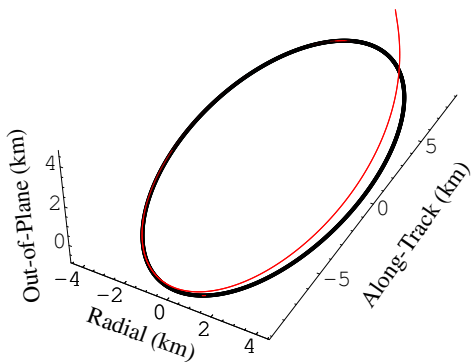
Note that while the control expression in Eq. (59) takes advantage of the linear mapping $A(\mathbf{e})$ between orbit element differences and their corresponding LVLH Cartesian coordinates, the control expression in Eq. (54) does not rely on this mapping. In fact, the relative orbit tracking errors $\Delta \mathbf{x}$ and $\Delta \mathbf{v}$ could be computed using the complete nonlinear mapping between orbit elements and local Cartesian coordinates. Further, it is possible to incorporate the J_2 effect here by using Brouwer's theory to compute the relative orbit errors in mean element space and then map the error vector back to osculating space for control purposes. The following numerical simulations will demonstrate the performance and limitations of either control law.

Numerical Simulations

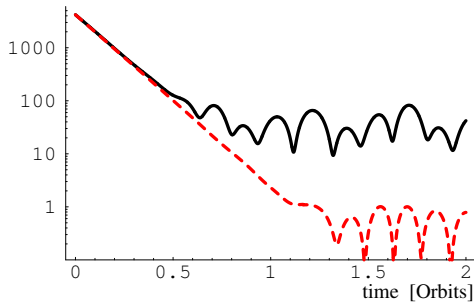
The performance of the two continuous feedback control laws in Eqs. (54) and (59) is illustrated through the following numerical simulations. Case 1, shown as a solid line in the figures, uses the simplified control in Eq. (59) which computes the tracking errors in osculating orbit space and takes advantage of the linear mapping between orbit element differences and their corresponding LVLH Cartesian coordinates. Case 2, shown as a dashed line in the figures, uses the more general control expression in Eq. (54). Instead of using the linear mapping, the relative orbit errors are computed using the complete nonlinear mapping between orbit elements and Cartesian coordinates. The development of the control law in Eq. (54) makes no assumption on whether the orbit elements and Cartesian coordinates are osculating or mean quantities. Therefore case 2 uses Brouwer's first order artificial satellite theory¹⁷ to compute any orbit errors in mean element space. The control in case 2 will thus ignore the J_2 induced short term oscillations and should provide a higher performing control algorithm than case 1.

Table 2 Deputy Orbit Element Differences

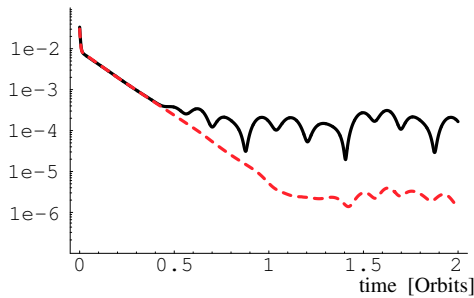
Orbit Element Difference	Value	Units
δa	1.92995	m
δe	0.000576727	
δi	0.00600	deg
$\delta \Omega$	0.0	deg
$\delta \omega$	0.0	deg
δM	0.0	deg



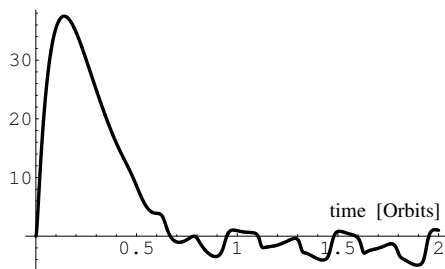
a) Relative Orbit shown in Chief LVLH Frame



b) Tracking Error (m)



c) Control Magnitude (m/s)



d) Tracking Error Difference (m)

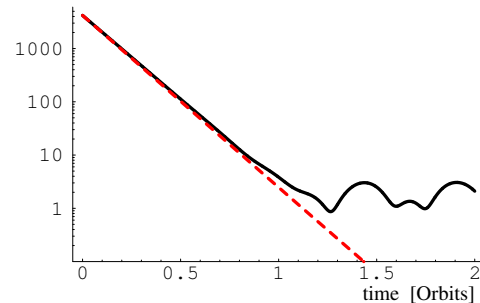
Fig. 2 Simulation Results including the J_2 through J_5 Zonal Harmonics

The chief satellite orbit has the mean orbit elements shown in Table 1. A J_2 -invariant relative orbit is designed using the two constraints developed in References 1 and 4. Prescribing an inclination angle difference of 0.06 degrees, the necessary δa and δe are shown in Table 2. The remaining three orbit element differences are set to zero. Initially, the deputy orbit has a relative orbit error of $\delta a = -0.1$ km, $\delta i = 0.05$ degrees and $\delta \Omega = -0.01$ degrees. The position and velocity feedback matrices K and P are replaced with the scalar gains

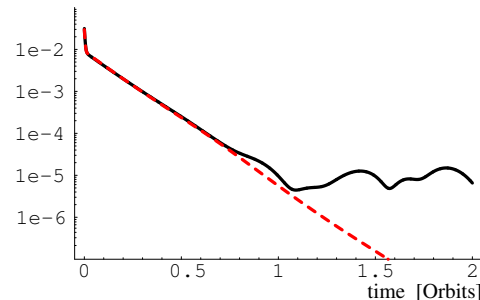
$$K = 0.000032 \text{ sec}^{-2}$$

$$P = 0.03 \text{ sec}$$

The numerical simulation solves the nonlinear equations of motion of each satellite including the J_2 through J_5 zonal harmonics. The results are shown in Figure 2. The initial relative orbit tracking error is over 1 kilometer. Figure 2(a) illustrates the relative orbit dictated by the desired relative orbit element differences shown in Table 2. This illustration shows the tracking error being essentially canceled after 0.5 orbits. Control cases 1 and 2 do not distinguish themselves at this scale and their performance difference cannot be observed here. Figure 2(b) shows the magnitude of the relative orbit tracking error on a logarithmic scale. For the first half orbit, both control cases perform in a near identical manner. This portion of the control maneuver is dominated by the feedback portion of the tracking errors. The tracking error for case 1 stabilizes about a mean value in the ten's of meters range. The Δv demanded for this two orbit maneuver is 9.98382 m/s. The tracking error for case 2 decays to a much smaller value of less than 1 meter with a commanded Δv of 8.42372 m/s. To isolate the cause for this performance improvement, another case 3 was run where the nonlinear transformation is used to map orbit element differences into corresponding LVLH Cartesian coordinates, but the tracking errors are computed in osculating element space, not in mean element space as is done in case 2. The tracking error difference between case 1 and this new case 3 is shown in Figure 2(d). Using the nonlinear mapping does result in a slightly better tracking performance initially. However, both case 1 and 3 stabilize on the same relative orbit tracking error. This indicates that the reduction in final tracking error in case 2 is due to computing the relative orbit tracking error in mean element space. Using the linear mapping $A(e)$ instead of the nonlinear mapping thus only causes a relatively minor transient tracking performance loss. To improve the steady state tracking error, it is necessary to operate in mean element space.



a) Tracking Error (m)



b) Control Magnitude (m/s)

Fig. 3 Simulation Results of Case 1 and Case 2 Using Keplerian Dynamics

To see the performance of the controls in Eqs. (54) and (59) without the J_2 gravitational perturbation, another set of numerical simulations was performed. No zonal harmonics are included in these simulations. The desired relative orbit is determined through the orbit element differences shown in Table 2, with the exception of $\delta a = 0$ km. This is

necessary for the relative orbit not to have a secular drift. A non-zero δa would cause the Keplerian orbits to have different orbit periods. The resulting relative orbit shape is essentially the same as the one shown in Figure 2(a). Note that the only difference between case 1 and case 2 test runs is that case 2 uses the nonlinear mapping between LVLH Cartesian coordinates and orbit element differences. Without gravitational perturbations present, the notion of osculating and mean element space has no meaning. These simulations illustrate the performance penalty of using the $A(e)$ matrix under the most ideal circumstances.

Figure 3 shows the simulation results for this Keplerian motion case. Note that the relative orbit tracking errors are reduced to a lower level in case 1 than they were with J_2 gravitational perturbations included. The steady-state tracking errors hover around the 1 meter point. The fuel consumed for the maneuver in case 1 is $\Delta v = 8.46227 \text{ m/s}$. If the nonlinear mapping is employed, than the tracking errors asymptotically decay to zero as predicted in the control analysis. The fuel consumed for case 2 is $\Delta v = 8.38649 \text{ m/s}$.

The linear mapping $A(e)$ provides a convenient method to map between the orbit element differences (which describe the relative orbit) and the LVLH Cartesian coordinates (which are likely to be the measured quantities). The error introduced through this simplification causes only a small loss in performance of typical control laws.

Conclusion

When describing and controlling natural (i.e. control-free) relative orbits, it is convenient to describe the desired relative orbit geometry in terms of orbit element differences. However, the actual relative orbit of a deputy satellite relative to a chief satellite will likely be measured in terms of Cartesian coordinates in the rotating chief LVLH frame. A direct linear mapping between the local Cartesian coordinates and the corresponding orbit element differences is outlined here. This mapping is used in the construction of a hybrid continuous feedback control law. The term hybrid is used here since the desired orbit is explicitly expressed in terms of orbit element differences, while the actual orbit measurements are provided in terms of LVLH Cartesian coordinates. Numerical simulations illustrate that the performance loss due to using the linear mapping is minimal. A more general form of the feedback control law also allows the relative orbit errors to be computed using the full nonlinearities of the relative orbit dynamics. In particular, the nonlinear mapping between Cartesian coordinates and orbit element differences, as well as the transformation from osculating to mean orbit element space, can be incorporated. The latter shows a substantially improved performance if the J_2 gravitational perturbation is included.

References

- ¹Schaub, H. and Alfriend, K. T., " J_2 Invariant Reference Orbits for Spacecraft Formations," *Flight Mechanics Symposium*, Goddard Space Flight Center, Greenbelt, Maryland, May 18-20 1999, Paper No. 11, to appear in the *Journal of Celestial Mechanics*.
- ²Vadali, S. R., Alfriend, K. T., and Vaddi, S., "Hill's Equations, Mean Orbit Elements, and Formation Flying of Satellites," *The Richard H. Battin Astrodynamics Conference*, College Station, TX, March 2000, Paper No. AAS 00-258.
- ³Chichka, D. F., "Dynamics of Clustered Satellites via Orbital Elements," *AAS/AIAA Astrodynamics Specialist Conference*, Girdwood, Alaska, August 1999, Paper No. AAS 99-309.
- ⁴Alfriend, K. T. and Schaub, H., "Dynamics and Control of Spacecraft Formations: Challenges and Some Solutions," *The Richard H. Battin Astrodynamics Conference*, College Station, TX, March 2000, Paper No. AAS 00-259.
- ⁵Carter, T. E., "State Transition Matrix for Terminal Rendezvous Studies: Brief Survey and New Example," *Journal of Guidance, Navigation and Control*, 1998, pp. 148-155.
- ⁶DeVries, J. P., "Elliptic Elements in Terms of Small Increments of Position and Velocity Components," *AIAA Journal*, Vol. 1, No. 1, Nov. 1963, pp. 2626-2629.
- ⁷Garrison, J. L., Gardner, T. G., and Axelrad, P., "Relative Motion in Highly Elliptic Orbits," *AAS/AIAA Spaceflight Mechanics Meeting*, Albuquerque, NM, Feb. 1995, Paper No. 95-194.

- ⁸Schaub, H. and Alfriend, K. T., "Hybrid Cartesian and Orbit Element Feedback Law for Formation Flying Spacecraft," *AIAA Guidance, Navigation and Control Conference*, Denver, CO, Aug. 2000, Paper No. 2000-4131.

- ⁹Alfriend, K. T., Schaub, H., and Gim, D.-W., "Gravitational Perturbations, Nonlinearity and Circular Orbit Assumption Effect on Formation Flying Control Strategies," *AAS Guidance and Control Conference*, Breckenridge, CO, February 2000, Paper No. AAS 00-012.

- ¹⁰Schaub, H., Vadali, S. R., and Alfriend, K. T., "Spacecraft Formation Flying Control Using Mean Orbit Elements," *AAS/AIAA Astrodynamics Specialist Conference*, Girdwood, Alaska, Aug. 16-19 1999, Paper No. 99-310, to appear in the *Journal of Astronautical Sciences*.

- ¹¹Schaub, H. and Alfriend, K. T., "Impulsive Spacecraft Formation Flying Control to Establish Specific Mean Orbit Elements," *AAS/AIAA Spaceflight Mechanics Conference*, Clearwater, Florida, Jan. 24-26 2000, Paper No. 00-113.

- ¹²Kapila, V., Sparks, A. G., Buffington, J. M., and Yan, Q., "Spacecraft Formation Flying: Dynamics and Control," *Proceedings of the American Control Conference*, San Diego, California, June 1999, pp. 4137-4141.

- ¹³Middour, J. W., "Along Track Formationkeeping for Satellites With Low Eccentricity," *Journal of the Astronautical Sciences*, Vol. 41, No. 1, Jan.-March 1993, pp. 19-33.

- ¹⁴Tan, Z., Bainum, P. M., and Strong, A., "The Implementation of Maintaining Constant Distance Between Satellites in Elliptic Orbits," *AAS Spaceflight Mechanics Meeting*, Clearwater, Florida, Jan. 2000, Paper No. 00-141.

- ¹⁵Melton, R. G., "Time-Explicit Representation of Relative Motion Between Elliptical Orbits," *Journal of Guidance, Control, and Dynamics*, Vol. 23, No. 4, 2000, pp. 604-610.

- ¹⁶Mukherjee, R. and Chen, D., "Asymptotic Stability Theorem for Autonomous Systems," *Journal of Guidance, Control, and Dynamics*, Vol. 16, Sept.-Oct. 1993, pp. 961-963.

- ¹⁷Brouwer, D., "Solution of the Problem of Artificial Satellite Theory Without Drag," *The Astronautical Journal*, Vol. 64, No. 1274, 1959, pp. 378-397.

Appendix

The inverse of the matrix $A(e)$ is presented in this appendix.⁹ To simplify the expressions, the following notation is introduced:

$$\begin{aligned} \alpha &= \frac{a}{R} & \nu &= \frac{V_r}{V_t} \\ \kappa_1 &= \alpha \left(\frac{p}{R} - 1 \right) & \kappa_2 &= \alpha \nu^2 \frac{p}{R} \end{aligned}$$

The non-zero matrix elements are given by:

$$A_{11}^{-1} = 2\alpha(2 + 3\kappa_1 + 2\kappa_2) \quad (61a)$$

$$A_{12}^{-1} = \frac{2\alpha^2\nu p}{V_t} \quad (61b)$$

$$A_{13}^{-1} = -2\alpha\nu(1 + 2\kappa_1 + \kappa_2) \quad (61c)$$

$$A_{14}^{-1} = \frac{2a}{V_t}(1 + 2\kappa_1 + \kappa_2) \quad (61d)$$

$$A_{23}^{-1} = \frac{1}{R} \quad (61e)$$

$$A_{25}^{-1} = (\cos\theta + \nu\sin\theta)\frac{\cot i}{R} \quad (61f)$$

$$A_{26}^{-1} = -\frac{\sin\theta\cot i}{V_t} \quad (61g)$$

$$A_{35}^{-1} = \frac{\sin\theta - \nu\cos\theta}{R} \quad (61h)$$

$$A_{36}^{-1} = \frac{\cos\theta}{V_t} \quad (61i)$$

$$A_{41}^{-1} = (3\cos\theta + 2\nu\sin\theta)\frac{p}{R^2} \quad (61j)$$

$$A_{42}^{-1} = \frac{p\sin\theta}{RV_t} \quad (61k)$$

$$A_{43}^{-1} = -\frac{1}{R}\left(\frac{p}{R}\nu^2\sin\theta + q_1\sin 2\theta - q_2\cos 2\theta\right) \quad (61l)$$

$$A_{44}^{-1} = \frac{p}{RV_t}(2\cos\theta + \nu\sin\theta) \quad (61m)$$

$$A_{45}^{-1} = -\frac{q_2\cot i}{R}(\cos\theta + \nu\sin\theta) \quad (61n)$$

$$A_{46}^{-1} = \frac{q_2\cot i\sin\theta}{V_t} \quad (61o)$$

$$A_{51}^{-1} = \frac{p}{R^2}(3\sin\theta - 2\nu\cos\theta) \quad (61p)$$

$$A_{52}^{-1} = -\frac{p\cos\theta}{RV_t} \quad (61q)$$

$$A_{53}^{-1} = \frac{1}{R}\left(\frac{p}{R}\nu^2\cos\theta + q_2\sin 2\theta + q_1\cos 2\theta\right) \quad (61r)$$

$$A_{54}^{-1} = \frac{p}{RV_t}(2\sin\theta - \nu\cos\theta) \quad (61s)$$

$$A_{55}^{-1} = \frac{q_1\cot i}{R}(\cos\theta + \nu\sin\theta) \quad (61t)$$

$$A_{56}^{-1} = -\frac{q_1\cot i\sin\theta}{V_t} \quad (61u)$$

$$A_{65}^{-1} = -\frac{\cos\theta + \nu\sin\theta}{R\sin i} \quad (61v)$$

$$A_{66}^{-1} = \frac{\sin\theta}{V_t\sin i} \quad (61w)$$